Magnetism at surfaces and defects in icosahedral Al-Pd-Mn quasicrystals

M. Krajčí[1,2] and J. Hafner[2]
[1]*Institute of Physics, Slovak Academy of Sciences, Dúbravská Cesta 9, SK-84511 Bratislava, Slovak Republic*
[2]*Fakultät für Physik and Center for Computational Materials Science, Universität Wien, Sensengasse 8/12, A-1090 Wien, Austria*
(Received 31 August 2009; revised manuscript received 23 November 2009; published 21 December 2009)

In our recent work [Krajčí and Hafner, Phys. Rev. B **78**, 224207 (2008)] we have demonstrated that the ground state of bulk i-Al-Pd-Mn quasicrystals is nonmagnetic. Mn atoms located at specific sites can acquire a large magnetic moment if they have at least two Pd neighbors in the first coordination shell. Such configurations can be created by substitutional Al/Pd defects which can be formed at low energetic cost because at these sites the overlap between the pseudo-Mackay and Bergman clusters building the quasicrystalline structure leads to conflicting assignments of the chemical decoration. Besides the large magnetic moments formed on these special Mn sites, we have found a broad diffuse background of smaller magnetic moments on many different Mn atoms induced by the large Mn moments. In the present work we extend these investigations to magnetism at the five-fold surface of the quasicrystal and at isolated point defects with particular attention to the formation of induced moments. For the stable five-fold surface we find that Mn atoms located in the surface layer carry indeed large magnetic moments of up to 3 μ_B and that smaller magnetic moments (aligned both parallel and antiparallel to the surface moments) are induced at distances of up to 10 Å below the surface. We have considered three types of isolated point defects (and substitutional defects) around a Mn atom and investigated the formation of magnetic moments on the Mn atom and of induced moments on the surrounding sites. For both the magnetization induced below a magnetic surface and the magnetization induced around an Al/Pd substitutional defect, the induced moments show an irregular dependence on the distance from the inducing "source" moment, but a marked dependence on the location of the Mn atom in the occupation domain in six-dimensional hyperspace. Mn atoms with a large coordinate in perpendicular space show large induced moments. Based on the analysis of the local paramagnetic density of states we demonstrate that the formation of a large induced moment is caused by a large polarizability of these Mn atoms, which is related in turn to a rather loosely packed local environment. Per Mn atom, the sum of the source moment (created by a special substitutional defect in the bulk quasicrystal or by the reduced coordination of a Mn atom at the surface) and of the induced moments reaches values of 6 to 8 μ_B, i.e., much higher than the limit set by Hund's rule for the spin moment of a free Mn atom.

DOI: 10.1103/PhysRevB.80.214419 PACS number(s): 61.44.Br, 71.23.Ft, 75.50.Kj

I. INTRODUCTION

The search for an accurate atomic description of the structure of quasicrystals and attempts to understand the correlation between the structure and the outstanding physical properties of quasicrystals have been a challenge to theoretical physics ever since the discovery of this fascinating class of long-range ordered structures.[1] The most sophisticated models presently available are those for stable icosahedral quasicrystals. These idealized models allow to construct diffraction diagrams that compare to the experimental data almost as accurately as those of refined models for complex periodic structures.[2] However, recent work has demonstrated the need for a further structural refinement based on an analysis of the electronic and magnetic properties and on cohesive energy calculations, in addition to the diffraction data.[3]

A very illustrative example for the need to base a detailed structural analysis of quasicrystals on physical information beyond diffraction measurements is provided by the stable, long-range ordered *F*-type icosahedral quasicrystals of the Al-Pd-Re and Al-Pd-Mn class. These icosahedral phases are largely free of atomic disorder and phason strains even if produced by rapid solidification.[4] The atomic structure has been thoroughly studied by x-ray and neutron diffraction, extended x-ray absorption fine structure (EXAFS), and various techniques based on electron microscopy. The analysis of these data has led to the construction of a structural model based on triacontahedral atomic surfaces in the perpendicular subspace of the six-dimensional (6D) space,[5–8] to which we refer as the Katz-Gratias-Boudard (KGB) model. The topology of the quasicrystalline structure may be described in terms of interpenetrating pseudo-Mackay (*M*) and pseudo-Bergman (*B*) clusters decorating the even and odd nodes of a three-dimensional (3D) Penrose tiling (Ammann-Kramer tiling).[7,9–12] The chemical decoration of this structure is determined by the internal shell structure of the triacontahedral atomic surfaces located at the odd and even nodes and at the body-centered position of the 6D hypercubic lattice.[12,13]

The quasicrystals of the i-Al-Pd-Mn(Re) class show exceptional electronic and magnetic properties. They have a high residual resistivity, a negative temperature coefficient of the electrical resistivity, and a magneto– resistance similar to that of doped semiconductors. These properties are indicative for the existence of a very deep minimum in the electronic density of states (a "pseudogap") at the Fermi level.[14,15] The magnetic properties of i-Al-Pd-Mn quasicrystals (and those of other Mn containing quasicrystals) are perhaps even more puzzling. At low temperatures the magnetic susceptibility measured in a weak alternating field displays a peak at $T_f \leq 5$ K, demonstrating the existence of interactions between local magnetic moments. However, the Curie constant

 ©2009 The American Physical Society

is very small and, in accordance with nuclear magnetic resonance measurements, it was concluded that most Mn atoms are nonmagnetic, while a small fraction carries a large moment. The concentration of magnetic Mn atoms varies with chemical composition and thermal history of the sample.[1,16–18] Recently we have demonstrated[19] that the opening of a gap or pseudogap in the electronic spectrum of i-Al-Pd-Mn(Re) quasicrystals is due to the formation of a topological band gap related to the existence of chains of alternating Al and transition-metal (TM) atoms linking the centers of pseudo-Mackay (M) clusters. The investigation of the physical mechanism promoting the formation of a pseudogap has also demonstrated that it is mandatory to use a well-relaxed structural model as the basis of these calculations—if the relaxation is suppressed, the pseudogap turns out to be significantly less pronounced.

While the electronic properties of i-Al-Pd-Mn are strongly influenced by the quasicrystalline topology, we have very recently shown that the magnetic properties are tightly correlated with the chemical ordering.[20] We have demonstrated that a slight modification of the internal boundaries of the atomic surfaces separating the occupation domains of Pd and Al atoms in the KGB model leads to a lowering of the total energy and to a suppression of the magnetic moments on all Mn sites. This model represents the intrinsically nonmagnetic ground state relative to a large number of possible variants of the KGB model. It is interesting to point out that bounded fluctuations of the atomic surfaces in perpendicular space have already been suggested by de Boissieu *et al.*[2,21,22] on the basis of the analysis of the partial Pd structure factors derived from anomalous x-ray diffraction.

The existence of different concentrations of magnetic Mn sites in real i-Al-Pd-Mn quasicrystals[16,23] has been attributed to substitutional defects on special sites in the immediate neighborhood of Mn atoms.[20] At these specific sites Al atoms can be replaced by Pd at very low energetic cost and without violation of the building principles of the quasicrystalline structure in terms of a decoration of a 3D Penrose tiling with M and B clusters. A large magnetic moment is formed on Mn atoms with two or three Pd neighbors. The interaction between the d bands of Pd and Mn is repulsive and this leads to a shift of the Mn d states to lower binding energies and an increase in the local Mn d density of states (DOS) at the Fermi level. A local magnetic moment is formed if the local paramagnetic DOS exceeds the Stoner limit. These special sites are located at those regions of the quasiperiodic lattice where the building clusters of the quasicrystalline structure (the pseudo-Mackay and Bergman clusters) are linked along the three-fold axes. A second mechanism leading to the formation of a local magnetic moment is a loosely packed local environment of a Mn atom. Within the KGB model the Mn atoms located in the center of the M clusters have an irregular first coordination shell consisting of seven to nine Al atoms,[12] as confirmed by EXAFS experiments.[24] This irregular coordination can lead to a loose coordination around the central Mn atom.

Besides the large magnetic moments formed due to coordination defects and/or loosely packed Mn environments, smaller magnetic moments (lower than about 0.5 μ_B) were found also on other Mn sites. A magnetization on these sites exists only if much larger magnetic moments (around 2.5 μ_B) have been created by one of the mechanisms discussed above. The magnetic moments of Mn atoms in i-Al-Pd-Mn can be thus divided into two classes—the "source" magnetic moments caused by structural defects and the induced moments. The existence of the induced magnetic moments could explain why the experimentally observed magnetic moments in quasicrystals appear to be so large. The size of the moments can be estimated from an analysis of the temperature dependence of the nonlinear susceptibilities above the spin-glass freezing temperature. For icosahedral Al-Mn-Si Berger and Préjean[25] reported that the average spin per magnetic Mn atom is $S \sim 3.7$ (i.e., larger than the upper limit $\frac{5}{2}$ for the spin of a free Mn atom set by Hund's rule) and the concentration of magnetic atoms is 0.27%, whereas the nominal Mn concentration is 21%. Hippert *et al.*[16,23] studied the low-temperature dependence of the magnetic susceptibility in several samples of i-Al-Pd-Mn quasicrystals. Under the assumption that the spin S of magnetic Mn atoms is equal to $\frac{5}{2}$, i. e., that all magnetic Mn atoms have the maximal magnetic moment of 5 μ_B, they found for samples of various composition a fraction of magnetic Mn atoms varying from 0.044% to 2.32%. In our theoretical study[20] we achieved for i-Al-Pd-Mn quasicrystal a good agreement with the experimental average magnetic polarization, but the size of the largest local magnetic moments did not exceed 3 μ_B. Detailed results on the magnitude and concentration of the magnetic moments on Mn atoms in icosahedral Al-Pd-Mn alloys have also been reported by Fukamichi.[26] The concentration of magnetic Mn atoms is around 2% to 2.5% of the total content in Mn, the magnetic moments vary between 6 and 7.5 μ_B. The fact that the magnetic moments deduced from the nonlinear susceptibilities exceed the limit of 5 μ_B set by Hund's rule requires an explanation. It has been suggested that these large magnetic moments arise from ferromagnetically coupled pairs of nearest-neighbor Mn atoms[25] (which are, however, absent in all variants of the KGB model). As an alternative explanation the formation of giant effective magnetic moments as for Mn, Fe, or Co impurities in highly polarizable hosts such as Pd has been proposed.[26] The effective moments consist of the moment of the magnetic impurity plus the magnetization induced on the surrounding host atoms.

However, it is evident that significant differences exist between the mechanisms for the formation of induced moments in crystalline metallic hosts and in quasicrystals. The formation of an induced magnetization cloud surrounding the magnetic impurity is driven by the Ruderman-Kittel-Kasuya-Yoshida (RKKY) interaction mediated by the conduction electrons, leading to a damped oscillatory decay of the induced moments with increasing distance from the source moment.[27] In i-Al-Pd-Mn substantial induced moments are found only on the Mn atoms, sometimes large moments are induced at large distances from the source moment whereas other Mn atoms located at shorter distances display only very low moments or remain even nonmagnetic. The physical effects governing the distribution of the local moments have not been analyzed very thoroughly as yet. This is the first goal of the present work.

The second topic to be addressed here are the magnetic properties of the surfaces of i-Al-Pd-Mn. It is well known

that for itinerant magnets, the moments are strongly enhanced at the surface due to the reduced atomic coordination leading to a narrowing of the bands of electronic eigenstates. There have even been reports[28] that the free surfaces of paramagnetic compounds such as Co_2Y are ferromagnetic. A reduced coordination or a loosely packed environment of the Mn atoms has also been identified as one of the possible mechanism for the formation of magnetic moments in i-Al-Pd-Mn. The fivefold surface of i-Al-Pd-Mn has been shown to be bulk terminated and to expose Mn atoms in low-coordinated sites. This suggests that large magnetic moments could also be found on these surfaces.

Our paper is organized as follows: In Sec. II the structural models of i-Al-Pd-Mn and of its five-fold surface are presented. Section III characterizes their electronic structures. The magnetic properties of the fivefold surface are investigated in Sec. IV. Induced magnetic moments in the near-surface region and in the bulk are studied in detail in Sec. V and we summarize in Sec. VI.

II. STRUCTURAL MODEL OF I-AL-PD-MN QUASICRYSTAL: BULK AND SURFACE

Structures for rational approximants to the quasicrystalline structure of bulk i-Al-Pd-Mn have been constructed using the cut-and-projection technique in six-dimensional hyperspace according to the KGB model. In the KGB model the vertices of a hypercubic lattice in 6D space are decorated by three kinds of triacontahedral occupation domains: two large triacontahedra at the "even" and "odd" nodes and a smaller triacontahedron at the body-centered positions.[45] The triacontahedron at the odd nodes is truncated by its intersections with its images along the fivefold axes. The shell structure of the occupation domains defines the chemical ordering. Details of the model have been discussed in our previous studies.[12,20]

All our studies of the electronic and magnetic properties of i-Al-Pd-Mn were performed on a 2/1 approximant. This approximant consists of 544 atoms in a cubic unit cell with the lattice constant $a=20.31$ Å. The occupation domain in perpendicular space is centered at the (0.5, 0.5, 0.5) position. This leads to $P2_1\bar{3}$ space-group symmetry (No. 198) of the approximant. Because of the periodicity of the approximant the triacontahedral domains of the quasicrystal are replaced by a coarse-grained approximation, see Fig. 1. Each cubic grain corresponds to one atom. The figure shows cuts through the occupation domains. The entire occupation domain of the 2/1 approximant consists of eleven layers indexed by $l=-5,\ldots,5$. A complete picture is shown in Fig. 3 of our previous paper.[20] In Fig. 1 only the layers containing Mn atoms are shown.

The internal shell structure of the occupation domains determines the chemical decorations of the sites. For our present studies we have chosen the chemical decoration corresponding the lowest total energy and a completely nonmagnetic state. In our previous study[20] this model is referred to as model B.

The atomic positions can be grouped into orbits (Wyckoff positions) with multiplicity 12 (a general position) or four (a

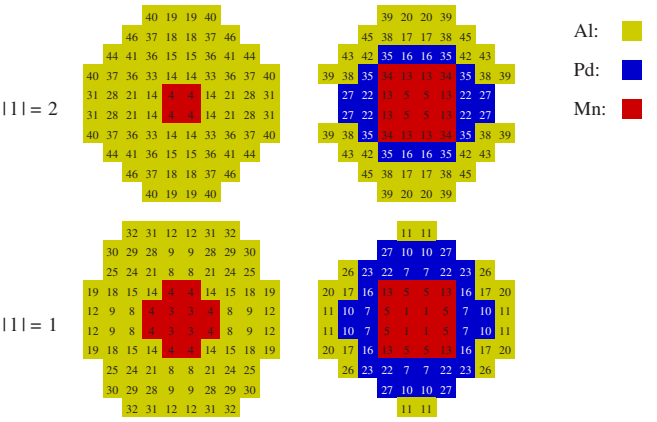

FIG. 1. (Color online) Cuts through the occupation domains of the Katz-Gratias-Boudard (KGB) model of the 2/1 approximant to quasicrystalline i-Al-Pd-Mn. The internal structure of the domains determines the chemical identity of atoms. Because of the periodicity of the approximant the triacontahedral shape of the domains of a quasicrystal is replaced by a coarse-grained approximation. Each grain corresponds to one atom. The inscribed numbers refer to the atomic orbits. Only the sections for $l=\pm 1, \pm 2$ containing Mn atoms are shown. Left-"even," right-"odd" motif.

position on the body diagonal which is a threefold symmetry axis). The 2/1 approximant has 50 inequivalent orbits. As all atoms belonging to the same orbit have identical local environments, the classification of the atoms by the orbit index is very useful for the discussion of the local electronic structure and magnetic moments. The numbers labeling the grains of the occupation domains in Fig. 1 define the orbits to which each atom belongs. The ground-state configuration (model B) found in our previous study[20] differs from the model with ideal triacontahedral occupation domains only in the occupation of orbits 17 and 42 where Pd atoms have been replaced by Al. With this chemical decoration each Mn atoms has at most one Pd nearest neighbor.

In the 2/1 approximant there are 48 Mn atoms grouped into 6 orbits. The center of the even node contains Mn atoms from orbits 3 and 4. The central part of the odd node is occupied by Mn atoms from orbits 1, 5, 13, and 34, see Fig. 1. In perpendicular space Mn atoms differ by their perpendicular coordinate Q_{perp} defined as a distance from the center of the occupation domain to the position of the Mn atom in the occupation domain. In Sec. V it will be demonstrated that Q_{perp} is closely related to the magnetic polarizability and the size of induced magnetic moments on the Mn atoms. Mn atoms from the orbits 1 and 3 have the smallest Q_{perp}. The central Mn domain of the odd node which in the KGB model of an infinite quasicrystal has the shape of the triacontahedron adopts in the 2/1 approximant the shape of a cube. Mn atoms from the orbit 34 are in the corners of the cube and thus have the largest perpendicular coordinate Q_{perp}.

In real space Mn atoms occupy the centers of the pseudo-Mackay clusters and vertex positions of an icosahedron in its second neighbor shell. In the KGB model there are no Mn-Mn nearest neighbors. In the model with ideal coordinates the shortest distances between Mn atoms are oriented along the five-fold axes and they are equal to the quasilattice

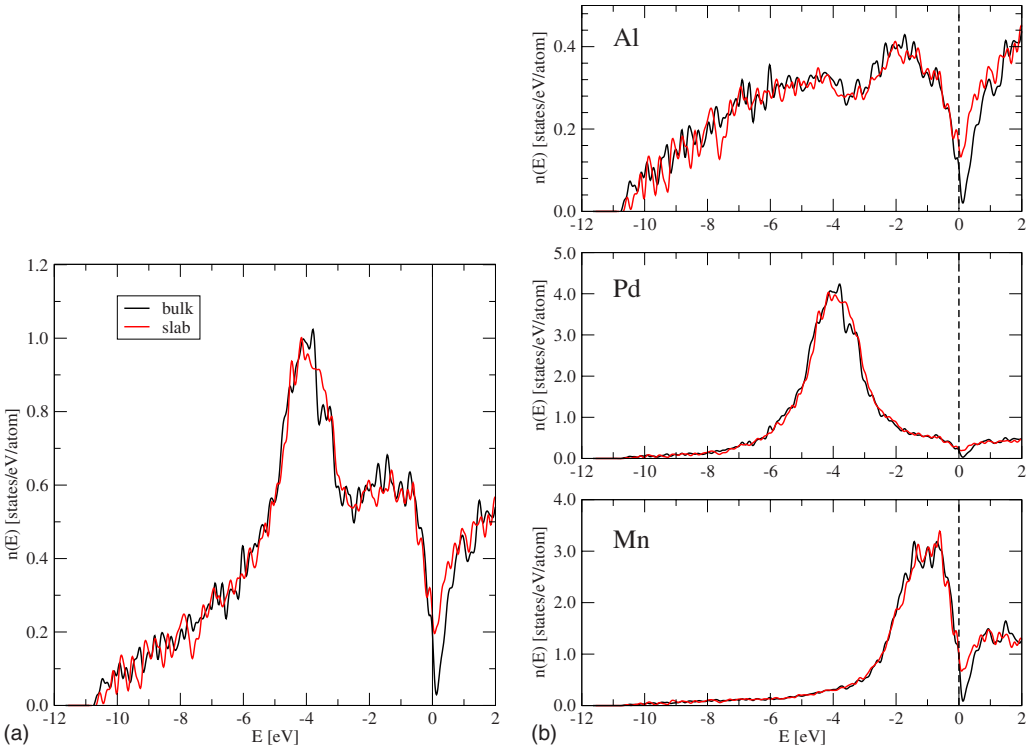

FIG. 2. (Color online) Total (a) and partial (b) DOS's of bulk i-Al-Pd-Mn (black) compared to those of the slab representing the fivefold surface (red, gray lines). The most remarkable feature of the DOS of bulk i-Al-Pd-Mn is the existence of a very deep and narrow pseudogap with a minimum slightly above the Fermi level. At the surface the pseudogap becomes partially filled.

constant of 4.56 Å. In the ideal model all Al-Mn bonds have the length of 2.57 Å and they are oriented along the threefold axes.

Structural model of the fivefold surface

Our model for the five-fold i-Al-Pd-Mn surface consists of a slab cut from the bulk quasicrystal, see Sec. II. The termination plane was chosen such that the quasicrystal is cleaved between the planes with the largest interlayer separation and that the surface exposes a tightly packed atomic layer, details are discussed in our previous papers.[29–31] The thickness of the slab is 13.1 Å and it consists of 19 atomic layers. The surface layer is Al-rich and contains a few ($\approx$4%) Mn atoms, but no Pd.[32] In our slab model this layer contains 39 Al atoms and 2 Mn atoms. The second atomic layer is located only 0.48 Å below the surface layer, it consists of 15 Pd and 9 Al atoms. In the i-Al-Pd-Mn quasicrystal there exist also fivefold atomic planes richer in Mn atoms than the top plane. We have chosen such a plane for the lower termination of our slab model. The bottom atomic plane consists of 37 Al atoms and 6 Mn atoms. In principle such an atomic plane could also appear as a real surface plane, but as the distance to the adjacent layers is smaller we expect it to have a higher surface energy. In addition to the outer atomic layers 1 and 19 Mn atoms are located also in planes 5, 7, 10, 13, and 16. All other atomic layers consist of Al and/or Pd atoms only. The thickness of the slab used in the present study is substantially larger than in models that we used in our previous studies of the adsorption properties of quasicrystalline surfaces.[29–31] The coordinates of all atoms in the slab were relaxed using interatomic forces calculated according to the Hellmann-Feynman theorem. The thickness of the slab proved to be sufficient to stabilize both surfaces, while in the inner layers the structure is hardly changed with respect to the bulk.

III. ELECTRONIC STRUCTURE OF I-AL-PD-MN: BULK AND SURFACE

Spin-polarized electronic structure calculations for both bulk and surface have been performed using the Vienna *ab initio* simulation package (VASP).[33–35] VASP produces an iterative solution of the Kohn-Sham equations of density-functional theory (DFT) within a plane-wave basis. The basis set contained plane waves with a kinetic energy up to 400 eV. The semilocal exchange-correlation functional in the generalized gradient approximation (GGA) proposed by Perdew *et al.*[36,37] and the spin-interpolation introduced by Vosko *et al.*[38] have been used. Prior to the calculation of the electronic spectrum and of the local magnetic moments the atomic structure was relaxed using a quasi-Newton technique and the Hellmann-Feynman forces acting on the atoms. For all further computational details we refer to our previous publications.[20,31]

Figure 2 displays the total and partial densities of states of bulk i-Al-Pd-Mn and of its fivefold surface. The most remarkable feature is the existence of a very deep and narrow pseudogap in the DOS with a minimum slightly (0.13 eV) above the Fermi level. The value of DOS in the minimum is

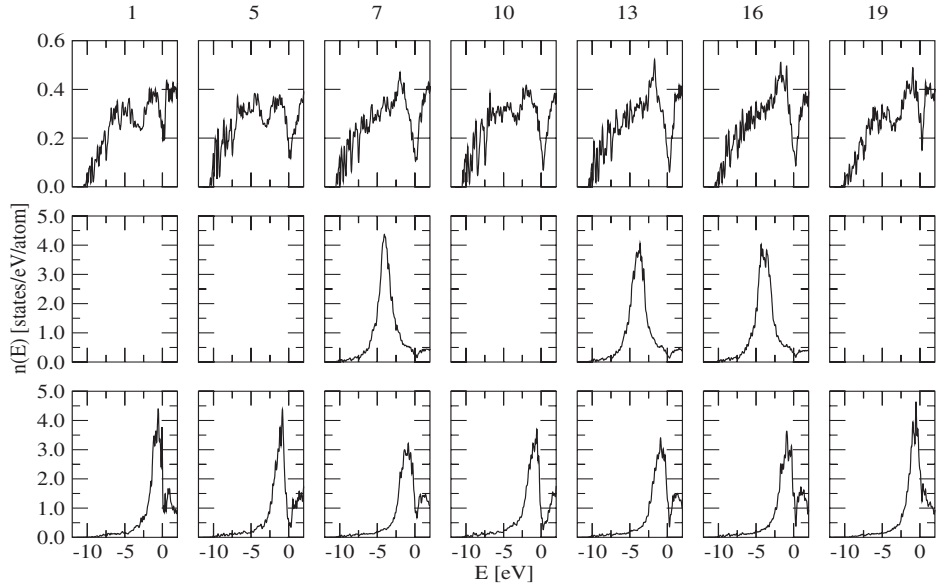

FIG. 3. The layer-decomposed partial DOS's in the slab used as a model for to the five-fold surface of i-Al-Pd-Mn. Only layers containing also Mn atoms are presented. The partial DOS's for Al, Pd, and Mn (from top to bottom) are averaged over the local DOS's of all atoms of the same species in the layer. The DOS minimum at the Fermi level is seen to be less pronounced at the surfaces (layers 1 and 19) for both Al and Mn atoms. At the surface, the Mn bands are narrower, the maximum of the DOS is increased.

0.03 states/eV/atom, i.e., only ≈8% of the DOS of face-centered cubic (fcc) Al at the Fermi level (0.37 states/eV/atom). At E_F the DOS is higher, $n(E_F)=0.20$ states/eV/atom. As a possible mechanism leading to the formation of such a deep pseudogap the existence of a network of linear chains of alternating Al and TM atoms extending along the twofold symmetry directions of the quasicrystal has been proposed.[19] The Al-TM chains link the centers of two *M* clusters along the short and long face diagonals of the Penrose rhombohedra. Note that the Al/TM alternation is also compatible with the chemical decoration of our model for the nonmagnetic ground state of i-Al-Pd-Mn. For the isostructural quasicrystal i-AlPdRe this mechanism explains the observed semiconducting properties.[19] The existence of the pseudogap near the Fermi level of i-Al-Pd-Mn has been confirmed by many experimental studies.[39–41] The presence of a deep pseudogap just above the Fermi level located on the steeply descending part of the DOS also has a substantial effect on the magnetic properties of the quasicrystal.

Electronic structure of the five-fold surface

In Fig. 2 the total and partial DOS's of the slab are compared with those of the bulk model. The only significant difference between the electronic spectra of bulk and surface is in the depth of the pseudogap at the Fermi level. Although the pseudogap of the slab model is still quite pronounced, it is significantly shallower than in the bulk. While the DOS minimum of the bulk is 0.03 states/eV/atom at an energy of 0.13 eV above E_F, the minimum of the surface DOS is 0.19 states/eV/atom at 0.08 eV. The shallower pseudogap can be attributed to the termination of the Al-TM chains at the surface.

Figure 3 shows the layer-decomposed partial DOS's in the atomic planes containing also Mn. The influence of the free surfaces on the electronic structure is clearly evident: (i) the depth of the pseudogap at E_F is reduced in both the Al- and Mn-partial DOS. In the Al-DOS it is deepest in layer 10 located near the center of the slab, it is much shallower in the surface layers 1 and 19. The Mn *d* states in the central plane 10 exhibit a clear minimum close to the Fermi level, but this splitting is much less pronounced at both surfaces of the slab. The splitting essentially disappears in the Mn-rich lower surface layer 19. (ii) The maximum of the Pd-DOS is located at a binding energy of about −4.5 eV, but still a small dip close to the Fermi level is observed, because Pd are also present on the characteristic Al-TM chains responsible for pseudogap formation. As the Pd-DOS at Fermi level is very low, the magnetic polarizability of the Pd atoms in i-Al-Pd-Mn is strongly reduced in comparison to pure Pd metal. (iii) The maximum of the Mn-DOS is located close to the Fermi level, at a binding energy of about −1 eV. In the surface layers the Mn bands are narrower than in the bulk, the DOS maximum is enhanced.

The deep pseudogap in the DOS observed in the bulk quasicrystal thus becomes less pronounced at the surface. A shallower pseudogap at the surface in comparison with the bulk has also been reported by Fourneé *et al.*[40] using photoelectron and Auger electron spectroscopies. They found that no pseudogap is observed on freshly cleaved five-fold surfaces of i-Al-Pd-Mn, but it can be restored by annealing or sputter annealing to sufficiently high temperatures.[40]

IV. MAGNETISM OF THE FIVE-FOLD I-AL-PD-MN SURFACE

In contrast to the nonmagnetic bulk, the five-fold surface of i-Al-Pd-Mn was found to be magnetic. Figure 4(a) shows

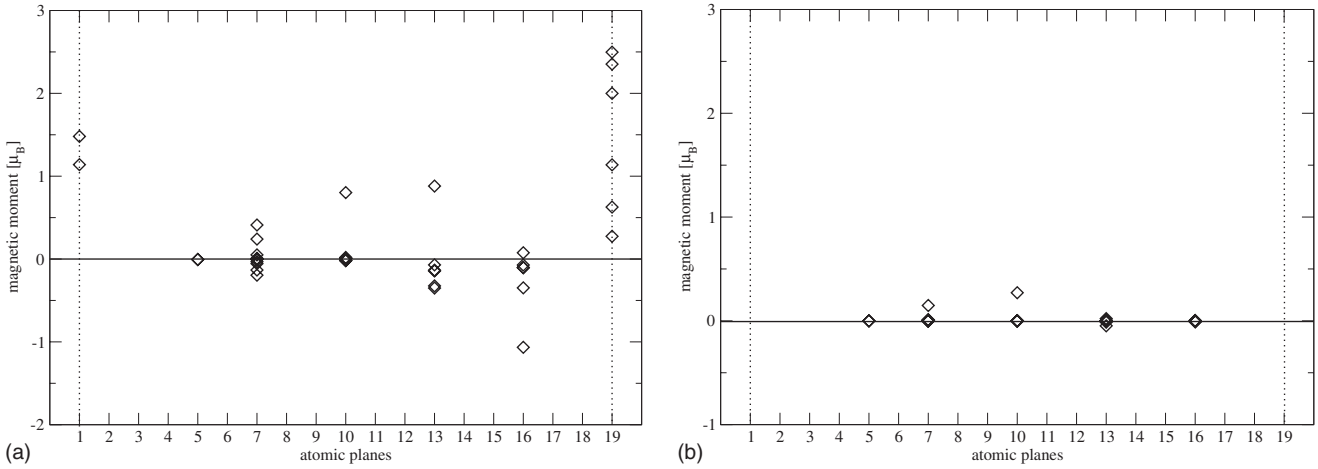

FIG. 4. Local magnetic moments of Mn atoms in the slab model of the fivefold surface of i-Al-Pd-Mn. (a) Although the slab was cut from a nonmagnetic bulk on Mn atoms at both surface layers 1 and 19 large magnetic moments appear. The magnetic moments on Mn atoms in the interior of the slab are induced by the magnetic polarization of the surface atoms. (b) If Mn atoms at both surface planes are removed the induced magnetic moments of the internal Mn atoms disappear almost completely.

the calculated local magnetic moments of the Mn atoms in the 19-layer slab. The majority of the Mn atoms are found to be magnetically polarized. The largest magnetic moments exist on the Mn atoms in both surface layers. At the surface with the lower Mn content (which has been found to correspond to the surface produced by cleaving), the local moments range between 1 and 1.5 μ_B. At the lower surface with a higher Mn content moments as large as 2.5 μ_B have been calculated, but for the reasons explained above we do not expect that this surface will be exposed on a real i-Al-Pd-Mn quasicrystal. Smaller magnetic moments are found also on most Mn located in the central layers of the slab, ranging from -1.06 μ_B to $+0.88$ μ_B. The existence of both positive and negative moments suggests that the magnetic moments of the Mn atoms on the inner layers might be induced by a RKKY interaction with the more strongly polarized Mn surface atoms.

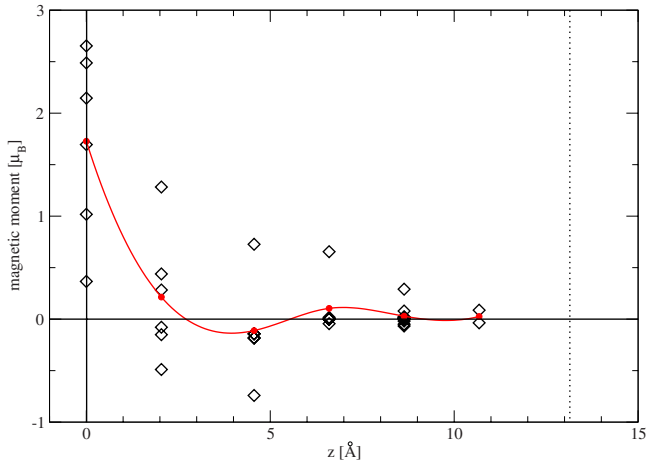

FIG. 5. (Color online) Magnetic moments in a model were Mn atoms were removed only from one side of the slab. The magnetic polarization extends up to $z \approx 10$ Å below the surface. The alternating signs of the induced magnetic moments suggest that the interaction has a damped oscillatory character. To visualize this dependence the average moments in each plane are connected by a smooth curve (red and gray).

To test this assumption we replaced the Mn atoms in the surface planes by Al atoms. After the substitution the coordinates of the atoms in the deeper layers of the slab were again relaxed, but the positions of the atoms in the surface layers had to be frozen because the substitution of Mn by Al destabilizes their atomic geometry. Figure 4(b) demonstrates that after replacing the magnetic Mn surface atoms by Al, the magnetic moments of the Mn atoms in the deeper layers have essentially vanished. This proves that these magnetic moments are indeed induced by the strong magnetic moments of the surface atoms. It is remarkable how deep the induced magnetic polarization penetrates below the surface. In Fig. 5 we show the magnetic moments calculated for a model were the Mn atoms were removed only from one side of the slab. The average magnetic moment per layer follows a damped oscillatory decay, the magnetic polarization extends up to $z \approx 10$ Å below the surface.

Hence, unlike the surface magnetism detected in crystalline intermetallic compounds,[28] the surface-induced magnetic polarization of i-Al-Pd-Mn extends rather deep into the bulk. If the strongly magnetic Mn surface atoms are eliminated, the magnetic polarization vanishes nearly completely. This suggests to distinguish—as in bulk i-Al-Pd-Mn containing magnetic Mn sites—between source and "induced" moments. At the fivefold surface of i-Al-Pd-Mn the source moments are created by the lower coordination of the Mn surface atoms. Thus the physical mechanism for the magnetic moments at the free surfaces is essentially identical to the mechanism for the formation of magnetic moments in the bulk at Mn sites with a loosely packed local environment. The conditions for moment formation through this mechanism will be discussed in more detail below. The induced magnetic moments are formed via a RKKY-like interaction. The Mn atoms interact via the free-electron-like Al and Pd s,p electrons. However, it has to be noted that the polarizability of the valence electrons is reduced by the presence of the pseudogap in the DOS. In the pure metal, the Pd-d states

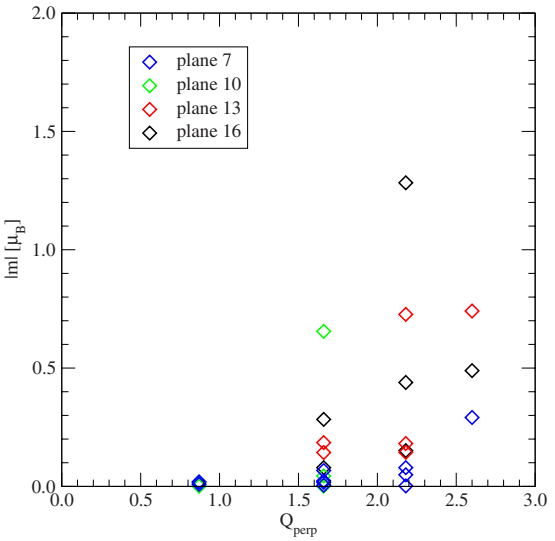

FIG. 6. (Color online) Correlation between the size of the induced moment and the position of the Mn atom in perpendicular space. Large induced magnetic moments are found only at sites with a large perpendicular coordinate Q_{perp}. Cf. text.

are also known to be highly polarizable. In the i-Al-Pd-Mn quasicrystal, however, the Pd-d band has been shifted to lower energies, leading to a strongly reduced polarizability. Hence the *d* states of the Pd atoms play only a minor role in the formation of induced magnetic moments, although they have been found to be very important for the formation of large Mn source moments.

In each atomic plane the magnitudes of the induced magnetic moments scatter significantly. The differences in the induced moments are related to their different distances from the source Mn atoms at the surface and to the different atomic environments of the Mn atoms in the quasicrystal. Interestingly, the dominant effect is not the distance from the source moment, but the local environment. This may be expressed in terms of a correlation between the size of the induced moment and the distance of the Mn atom from the center of the occupation domain in perpendicular space, see Fig. 6. No large induced magnetic moments exist at sites with a small perpendicular coordinate Q_{perp}. In Sec. V C it will be shown that the same correlation exists also in the bulk: the local electronic DOS and the magnetic polarizability of the Mn atoms are related to the coordinate of its image in perpendicular space.

Figure 7 shows the spin-polarized electronic *d* DOS's averaged over all Mn atoms in the same atomic layer of the slab model. The exchange splitting is largest for Mn atoms in the surface layer and nearly vanishes in the center of the slab. This suggests a Stoner-like correlation between local moment and exchange splitting.

This correlation is analyzed in detail in Fig. 8 which shows the local moment and the local exchange splitting of the Mn *d* bands, defined as the difference in the positions of the center of gravity of spin-up and spin-down bands. The correlation is strictly linear for source AND induced moments, the slope of the line yields a value of the Stoner parameter of $I=0.72$ eV/μ_B. Essentially the same value of

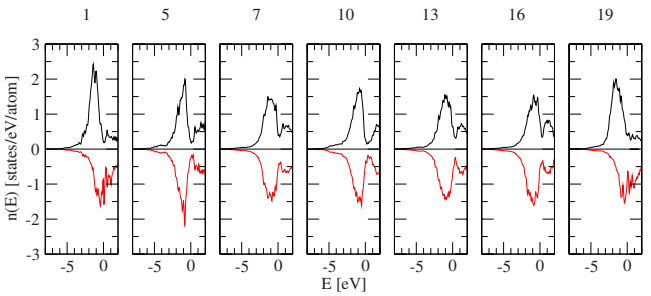

FIG. 7. (Color online) Spin-polarized *d*-electron DOS's averaged over Mn atoms in the atomic planes.

the Stoner parameter has been calculated for all different structural models of i-Al-Pd-Mn which display magnetic moments at a strongly varying concentration of magnetic Mn sites.[20] This correlation confirms the validity of the band model for the description of the magnetism in i-Al-Pd-Mn, in the bulk and at the surface.

V. SOURCE AND INDUCED MAGNETIC MOMENTS

The results of our investigations of surface-induced magnetism in i-Al-Pd-Mn have confirmed the difference in the physical mechanisms leading to the formation of the large source moments and the smaller induced moments. In our previous studies of magnetism in bulk quasicrystals[20] our attention was focused on the origin of the magnetic polarization of the Mn atoms carrying the largest magnetic moments. The origin of the magnetic moments smaller than 0.5 μ_B on other Mn sites was not investigated in detail. It was assumed that these small moments are caused by some kind of interaction with the strongly magnetic atoms, generally over distances larger than the nearest-neighbor shell.

Here we return to the question of the origin of the induced magnetic moments. Based on the structural model for the nonmagnetic ground state of the bulk quasicrystal we investigate the response of nonmagnetic but polarizable Mn atoms to the formation of a magnetic moment on a selected source

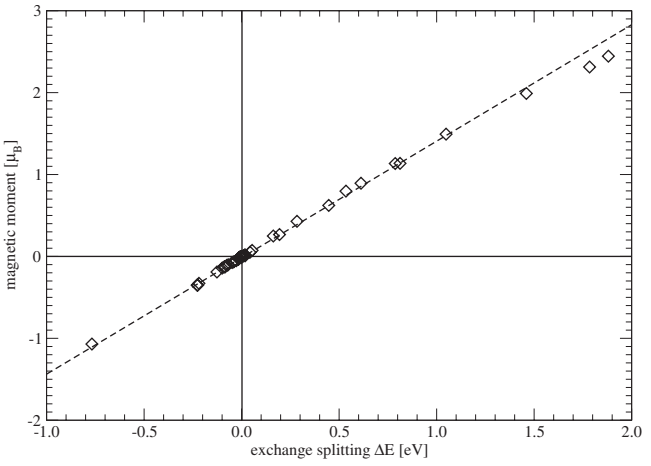

FIG. 8. Correlation between the local moments and the local exchange splitting of the *d* bands in the slab model of the fivefold surface of i-Al-Pd-Mn.

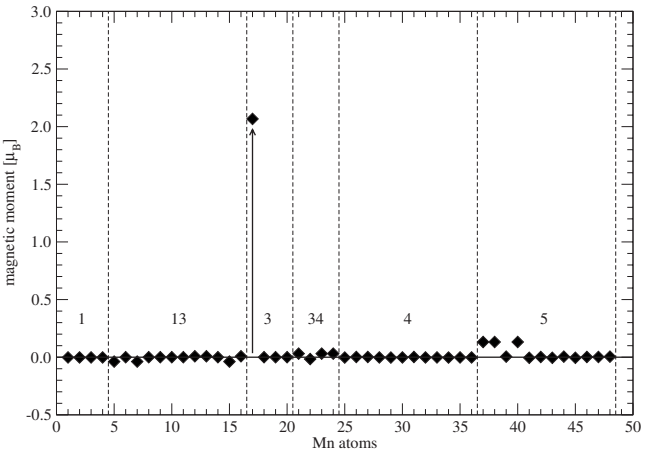

FIG. 9. Formation of a magnetic moment on a Mn site with a loosely packed local environment. At one selected atom, $Mn_{17}(3)$ (marked by an arrow), the coordinates of the seven nearest-neighbor Al atoms are fixed at their ideal values. This atom becomes strongly magnetically polarized. On three other Mn atoms small induced magnetic moments are found.

Mn atom. As demonstrated in our earlier study, the source magnetic moment can be created either by a loosely packed local environment or an increased Pd content in the nearest-neighbor shell of the Mn atoms. We shall investigate both cases.

A. Loosely packed Mn environment

The atomic structure of the i-Al-Pd-Mn quasicrystal can be interpreted in terms of interpenetrating pseudo-Mackay (M) and Bergman (B) clusters.[11,20] The Mn atoms in the center of the M clusters are known to have a low coordination. The nearest-neighbor shell contains only seven atoms and has an irregular structure, as confirmed by EXAFS studies.[24] On the five-fold surface, the low coordination of the center of the M clusters can lead to the creation of a surface vacancy if a cluster around a Mn atom in subsurface site is cut by the surface. The existence of such surface vacancies has been confirmed by combined modeling and scanning tunneling microscopy studies.[29,30] As the quasicrystalline structure is loosely packed around these sites it seems natural to assume that the Mn atoms in the centers of the M clusters carry large magnetic moments. However, as we have already demonstrated,[20] this is not the case for a real quasicrystal. Only in a model with idealized coordinates, which does not account for the smaller size of the Mn atoms, large moments are formed at the centers of the M clusters. If the positions of the atoms are allowed to relax to their equilibrium positions the magnetic polarization on all sites disappears completely (see Fig. 10 in Ref. 20). However, in our earlier study we have analyzed only two limiting cases. In the first relaxation was completely suppressed, all atoms occupy the positions determined by the projection from 6D space. In this case eight out of the 48 Mn atoms in the unit cell of the 2/1 approximant carry magnetic moments between 2 and 2.5 μ_B, and all other Mn atoms are also magnetic with moments close to 0.5 μ_B. All atoms belonging to the same orbit have the same moment. The second case is a completely relaxed model which has been found to be entirely nonmagnetic. The existence of a large fraction (16%) of strongly magnetic moments with overlapping induced magnetization clouds makes it almost impossible to unravel the mechanisms determining the formation of the smaller induced moments.

TABLE I. Magnetic moment of the source Mn atom and the total magnetization of the unit cell for different configurations with local defects (loosely packed environment and/or Al/Pd substitutions, see text). The numbers in the brackets are s, p, and d contributions to the magnetic moment.

Case	Source moment (μ_B)	Total moment (μ_B)
L1 (Fig. 9)	2.067(0.019,0.027,2.021)	2.06(−0.15,−0.12,2.33)
V1	0.130(0.001,0.004,0.125)	2.50(−0.12,−0.03,2.65)
V2	0.360(0.003,0.002,0.355)	2.10(−0.11,−0.09,2.31)
P1 (Fig. 10)	2.536(0.021,0.014,2.501)	6.05(−0.25,−0.15,6.45)
P2 (Fig. 12)	1.189(0.010,0.015,1.164)	8.35(−0.37,0.04,8.68)

Therefore we decided to construct a model were a large source moment is found only on a single Mn site. The 48 Mn atoms in the unit cell of the 2/1 approximant can be divided into 6 groups belonging to the orbits (Wyckoff positions) 1, 3, 4, 5, 13, and 34. In the ground state of the model with the relaxed coordinates all are nonmagnetic. For one selected atom, $Mn_{17}(3)$ (the number in parentheses denotes the orbit, the subscript merely numbers the Mn sites from 1 to 48), located in the center of a M cluster we have fixed the coordinates of its seven nearest-neighbor Al atoms at the ideal positions. The Al atoms are located at a distance of 2.56 Å from the central Mn atom, while around the $Mn_{18}(3)$-$Mn_{20}(3)$ atoms from the same orbit the Al neighbors are located at distances of 2.29 Å (four Al atoms) and 2.30 Å (three Al atoms).

Figure 9 shows that while at the site $Mn_{17}(3)$ with the loosely packed environment a large magnetic moment of 2.05 μ_B is formed, all other Mn atoms belonging to the same orbit 3 are essentially nonmagnetic. Small magnetic moments of 0.13 μ_B are induced at sites $Mn_{37}(5)$, $Mn_{38}(5)$, and $Mn_{40}(5)$ which are all located at a distance of 4.56 Å from the source moment.

Table I compares the values of the total magnetization per unit cell with the values of the source magnetic moments for all configurations where a local magnetic moment has been created by a structural defect. The model with a loosely packed environment around the $Mn_{17}(3)$ site is listed as case L1. The source and total magnetic moment as well as the contributions from s, p, and d states are listed. For configuration L1 the total magnetization of 2.06 μ_B is almost identical to the source moment of 2.067 μ_B because a positive induced magnetization of the d-states is compensated by negative contributions from s and p states of almost all Al and Pd atoms.

A configuration where relaxation has been suppressed around single atoms is certainly a bit artificial. However, at high temperatures similar loosely packed environments can

exist as a consequence of thermal fluctuations and thermal expansion. Indeed our observation that magnetic Mn atoms can exist in a loosely packed quasicrystalline environment correlates with the experimental finding that most Mn atoms in liquid AlMn or Al-Pd-Mn alloys carry a magnetic moment.[42] This also agrees with spin-density-functional calculations.[43,44]

A loosely packed environment of a Mn atom can also be created by the formation of a structural vacancy on a nearest-neighbor position. As in a quasicrystal there are many different possibilities to create a vacancy near a Mn atom, an exhaustive study would be very difficult. Therefore the three configurations we have examined might not represent a complete picture. In configuration V1 an Al vacancy was created in the first neighbor shell of the $Mn_{17}(3)$ atom. After the structural relaxation only a very modest magnetic moment of 0.13 μ_B was found on this atom. Surprisingly, the total magnetization of the cell of 2.50 μ_B was found to be substantially higher (see Table I). A similar result was found for configuration V2 where an Al atom was removed from the first neighbor shell of the $Mn_{24}(34)$ atom. The local magnetic moment on the $Mn_{24}(34)$ atom was 0.36 μ_B, while the total magnetic polarization of the unit cell is 2.10 μ_B. In a third case vacancy formation did not affect the nonmagnetic ground state at all after a careful structural relaxation (all vacancies lead to the formation of magnetic moments if the structure around the defect is not relaxed—but this would be an unrealistic configuration). Obviously during structural relaxation the atoms rearrange their positions in such a way that the free volume created by the removal of one atom is spread out over a wider environment. In both configurations V1 and V2 the main contribution to the increased total magnetization comes from Mn(34) atoms. Atoms located in these sites are highly polarizable. In Sec. V C it will be shown that their local densities of states at the Fermi level are very close to the threshold of the Stoner criterion for the formation of a local moment. A small modification of their environments can thus easily trigger a magnetic polarization of these atoms.

B. Substitutional defects—Mn-Pd nearest neighbors

For bulk i-Al-Pd-Mn we have demonstrated[20] that if a Mn atom has at least two nearest Pd neighbors, it acquires a substantial magnetic moment. In a structural model (labeled A) for the 2/1 approximant based on ideal triacontahedral occupation domains (respectively their coarse-grained approximations) eight Mn atoms belonging to orbits 4 and 34 have two, respectively, three Pd nearest neighbors belonging to orbits 17 and 42 (see Fig. 9 in Ref. 20). Only these Mn carry large source moments. Moment formation on these sites is driven by the repulsive interaction between the Mn and Pd d bands which leads to a shift of the Mn d band to lower binding energies and an increased local Mn d DOS at the Fermi level. According to the Stoner criterion for band magnetism a magnetic moment is formed if the local paramagnetic density of d states $n_d(E_F)$ is higher than a certain threshold of about ≈ 2 states/eV. The mechanism for the formation of the smaller induced moments cannot be explored in such a model, because the induced polarization clouds of the eight source moments overlap.

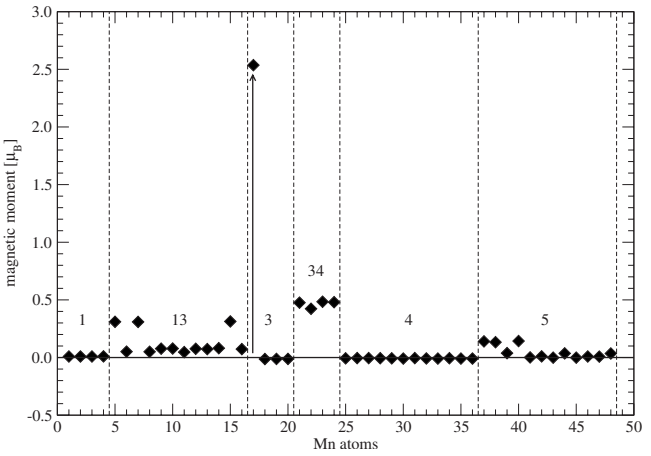

FIG. 10. Distribution of the magnetic moments in a model (configuration P1) where around one selected $Mn_{17}(3)$ atom (marked by an arrow) three Al nearest neighbors were replaced by Pd atoms. In addition to the large source moment created on this Mn atom smaller induced moments appear on other Mn sites—the total magnetic moment is 6.05 μ_B. Cf. text.

This is possible if we start from the nonmagnetic ground state of i-Al-Pd-Mn where orbits 17 and 42 are occupied by Al (note that in the quasiperiodic limit this amounts to a modification of the triacontahedral surface separating the Pd and Al shells of the occupation domain centered at the odd nodes in 6D space, see Fig. 1). In this model no Mn atom has more than one Pd neighbor. To create a source moment on a single Mn site we replaced in the nearest-neighbor shell of the $Mn_{17}(3)$ atom located in the center of a M cluster three Al atoms by Pd.

Figure 10 shows the magnetic moments of the Mn atoms in this model (called configuration P1). Only the $Mn_{17}(3)$ atom (marked by an arrow) shows a large magnetic moment of 2.54 μ_B created by the repulsive interaction between the Mn and Pd d bands described above. Smaller induced moments appear on other Mn sites belonging to different orbits, but their magnitude does not depend solely on the distance from the source moment, see Fig. 11(a). The reason is that in the Al-Pd-Mn quasicrystal different Mn atoms occur in different local environments, leading to large differences in their polarizability. We find that the magnitude of the induced moments (and therefore also the polarizability of the Mn atom) can be characterized by the coordinate Q_{perp} of the atom in perpendicular space. Q_{perp} measures the distance of a Mn atom from the center of the occupation domain, see Fig. 1. Figure 11(b) shows that the size of the moments induced on Mn atoms increases with increasing Q_{perp}. The total (source plus induced moments) magnetic moment of 6.05 μ_B is substantially larger than the moment of the source Mn atom, see Table I.

Figure 12 shows another example of a large source moment created by Mn-Pd nearest neighbors and the smaller moments induced by the source moment. In this model (labeled P2) we created a magnetic moment at the $Mn_{25}(4)$ atom (marked by an arrow) by replacing two of its Al nearest

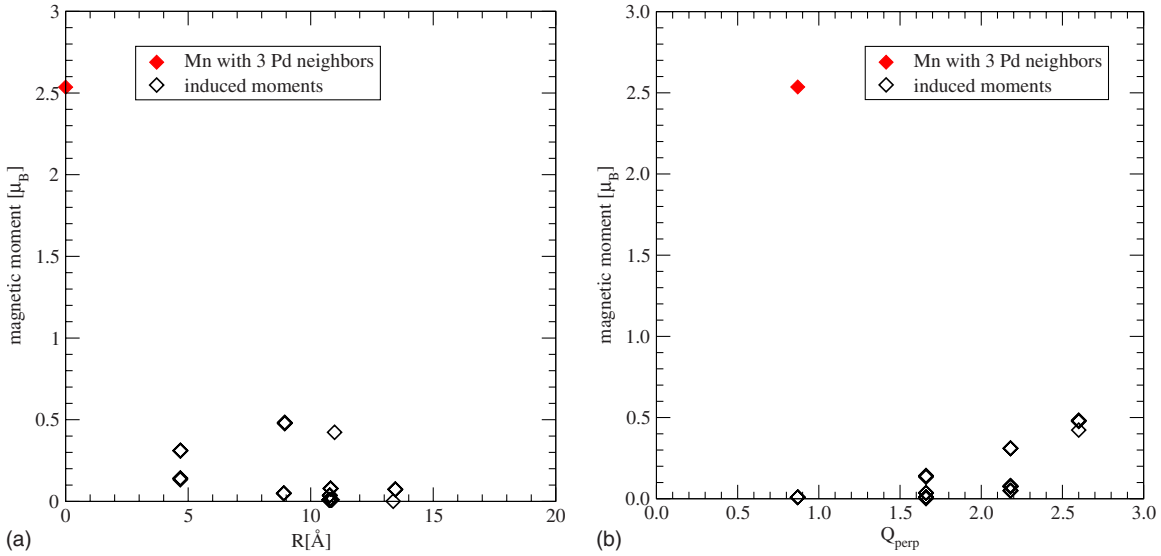

FIG. 11. (Color online) (a) Variation in the induced moments on Mn with their distance from the source Mn atom-configuration P1. (b) Correlation between the induced Mn moments and their coordinate Q_{perp} in perpendicular space measuring the distance from the center of the occupation domain.

neighbors by Pd atoms. The other Mn atoms have Al nearest neighbors only. The source moment created by the *d*-band repulsion on the $Mn_{25}(4)$ site is 1.21 μ_B. It is surprising that in this case the induced magnetic moments, particularly those on the atoms Mn(34), are almost as large as the source moment. Figure 13 demonstrates again that the magnitude of the induced moments is largely independent of the distance from the source atom, but varies strongly with increasing values of the perpendicular coordinate Q_{perp}. Mn atoms belonging to orbit 34 represent a special case—should they be considered as induced or as source moments? Our previous study has shown that even if all four Mn(34) atoms have three Pd nearest neighbors, a large source moment (≈ 2 μ_B) is created only if there is a Mn(4) atom on a next-nearest-neighbor position. If this site is occupied by an Al atom, only much lower magnetic moment of ≈ 0.5 μ_B is formed (compare models D and F in Ref. 20).

For configuration P2 the total magnetic moment is even 8.35 μ_B. Hence in both cases the effective magnetic moment per source Mn atom is much larger than the limit of 5 μ_B set by Hund's rule to the magnetic moment of a free Mn atom. Both examples show that the largest induced moments are found on Mn sites with large coordinates in perpendicular space—this suggests a correlation between the polarizability of the Mn atoms and the structure of the quasicrystal in 6D space.

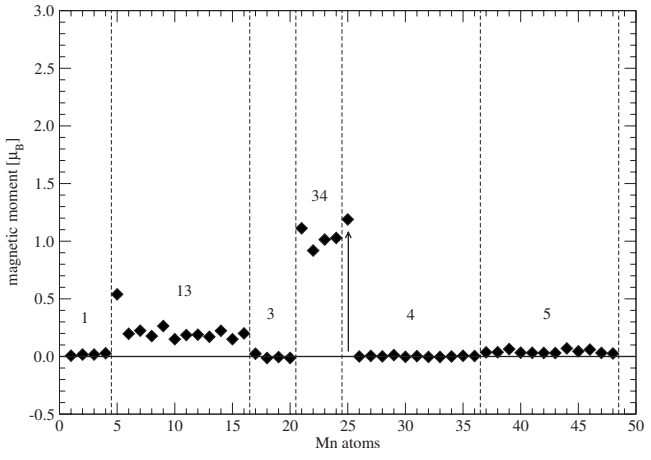

FIG. 12. Distribution of the magnetic moments in a model (configuration P2) where around the $Mn_{25}(4)$ atom (marked by an arrow) two Al nearest neighbors were replaced by Pd atoms. In addition to the large source moment created on this Mn atom smaller induced moments appear on other Mn sites—the total magnetic moment is 8.35 μ_B. Cf. text.

C. Mn polarizability and 6D geometry

The surprising correlation between the induced magnetic moments (and hence of the magnetic polarizability of the sites were the moments is created) and the coordinates of the sites in 6D space can be understood using an analysis of the local densities of states. Figure 14(a) compares the local *d* DOS on the $Mn_{17}(3)$ atom with 3 Pd neighbors (carrying the source moment) with that on the $Mn_{18}(3)$ (belonging to the same orbit) and on the $Mn_{21}(34)$ atom with the largest induced magnetic moment. Moment formation is determined by the Stoner criterion—a magnetic moment is formed on those sites where the local paramagnetic density of *d*-states $n_d(E_F)$ exceeds the critical value of ≈ 2 states/eV. The high value of the paramagnetic DOS at E_F of the $Mn_{17}(3)$ atom of ≈ 6.2 states/eV results from the *d*-band repulsion, it is responsible for the formation of the large source moment of 2.54 μ_B, see Fig. 10. At the $Mn_{18}(3)$ site [which is crystallographically equivalent in the absence of Al/Pd substitutions around the $Mn_{17}(3)$ site] the Fermi levels falls close to the minimum in the DOS and thus this atom is nonmagnetic. This illustrates that the formation of the source moment is indeed driven by the Mn-Pd interactions. The local *d*-DOS of

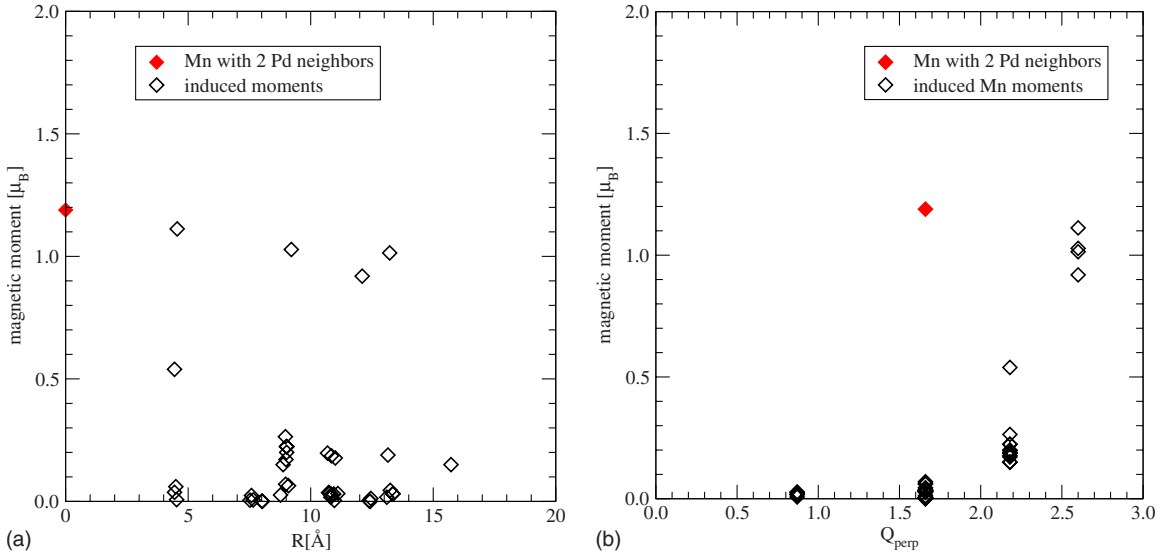

FIG. 13. (Color online) (a) Variation of the induced moments on Mn atoms with their distance from the source Mn atom—configuration P2. (b) Correlation between the induced Mn moments and their coordinate Q_{perp} in perpendicular space measuring the distance from the center of the occupation domain.

the $Mn_{21}(34)$ atom exhibits a side-peak close to the Fermi level, leading to a paramagnetic DOS of $n_d(E_F)=2.25$ states/eV is slightly higher than the Stoner limit. This Mn atom is thus magnetically polarizable and this explains its induced magnetic moment of $\approx 0.5\ \mu_B$.

The Mn atoms with nonzero induced magnetic moments in configuration P1 (see Fig. 10) belong to three atomic orbits: Mn(5), Mn(13), and Mn(34). Figure 14(b) compares the local paramagnetic *d*-electron DOS at these sites. All three have a minimum at ≈0.2 eV above E_F, but differ in their value at E_F. The local *d*-DOS of the Mn(34) atoms with the highest perpendicular coordinate of $Q_{perp}=2.60$ has a side peak at E_F while the local DOS's of Mn atoms with lower Q_{perp} exhibit only shoulders at this energy. The paramagnetic $n_d(E_F)$ and therefore also the magnetic polarizability increases with increasing Q_{perp}.

Figure 14(c) presents the same comparison for configuration P2 (see Fig. 12). Here the differences in the local *d*-DOS's at E_F are essentially the same, but their values are somewhat enhanced in comparison to configuration P1. The subpeak of $n_d(E)$ at E_F for the Mn(34) atoms with the highest Q_{perp} reaches even a value of ≈3 states/eV. These atoms are thus highly polarizable and therefore in Fig. 12 one observes high values of the induced magnetic moments. The small differences in the local DOS at the Mn(34) sites in configurations P1 and P2 at related to different distances between the Mn(34) sites and the source moment [see Figs. 11(a) and 13(a)]. In configuration P2 all Mn(34) sites lie at distances of 9 to 11 Å from the source moment, while in configuration P2 they are located at distances varying between 4.6 and 13 Å.

The polarizability of a Mn atom can be thus characterized by the perpendicular coordinate Q_{perp}—but this raises the question how the local atomic environment of a Mn atom in physical space depends on the location of its image in perpendicular space. The KGB model of i-Al-Pd-Mn has a shell structure of the occupation domains in the perpendicular space defining the chemical decoration of the quasicrystalline lattice. Mn atoms with small Q_{perp} close to the center of the even [Mn(3), Mn(4)] and odd [Mn(1), Mn(5)] occupation domains (see Fig. 1) correspond to the centers of *M* and *M′* clusters (there are two kinds of the *M* clusters corresponding to the even and odd domains, respectively). Mn atoms with large Q_{perp}, in particular those belonging to orbit 34, are located at the boundary to the Pd domains and occupy sites that could also by occupied by the much larger Pd atoms. Mn atoms located at such sites are thus highly polarizable. At these sites Mn atoms are on the threshold to become magnetically polarized because of a loosely packed local environment.

We have also observed that there is a direct relation between the minimal Al-Mn distance and the induced magnetic moment on a Mn atom. If around a Mn atom an Al atom is found at a distance of $d_{\text{Al-Mn}}=2.28-2.32$ Å then the Mn atom is always nonmagnetic. This is the case for the Mn(1) and Mn(3) sites with the lowest Q_{perp}. On the other hand, if the closest Al-Mn is larger than ≈2.50 Å then the Mn atom can be polarized very easily. This is the case for the Mn(34) sites with the largest Q_{perp} where the Mn-Al distances are about 2.9 Å in an idealized structure and even increase up to 3.1 Å upon relaxation.

A short Al-Mn distance indicates an enhanced covalency of the bonding. The Mn atoms from the center of the occupation domains participate in the formation of the partially covalently bonded Al-TM chains extending along the twofold symmetry directions of the quasicrystal. We have already demonstrated[19] that the strict Al/TM alternation along these chains is instrumental for the formation of the deep pseudogap in the DOS close to the Fermi level and hence for the outstanding electronic transport properties of these materials.

VI. DISCUSSION AND CONCLUSIONS

In the present work we have completed our *ab initio* investigations of the formation of magnetic moments on Mn

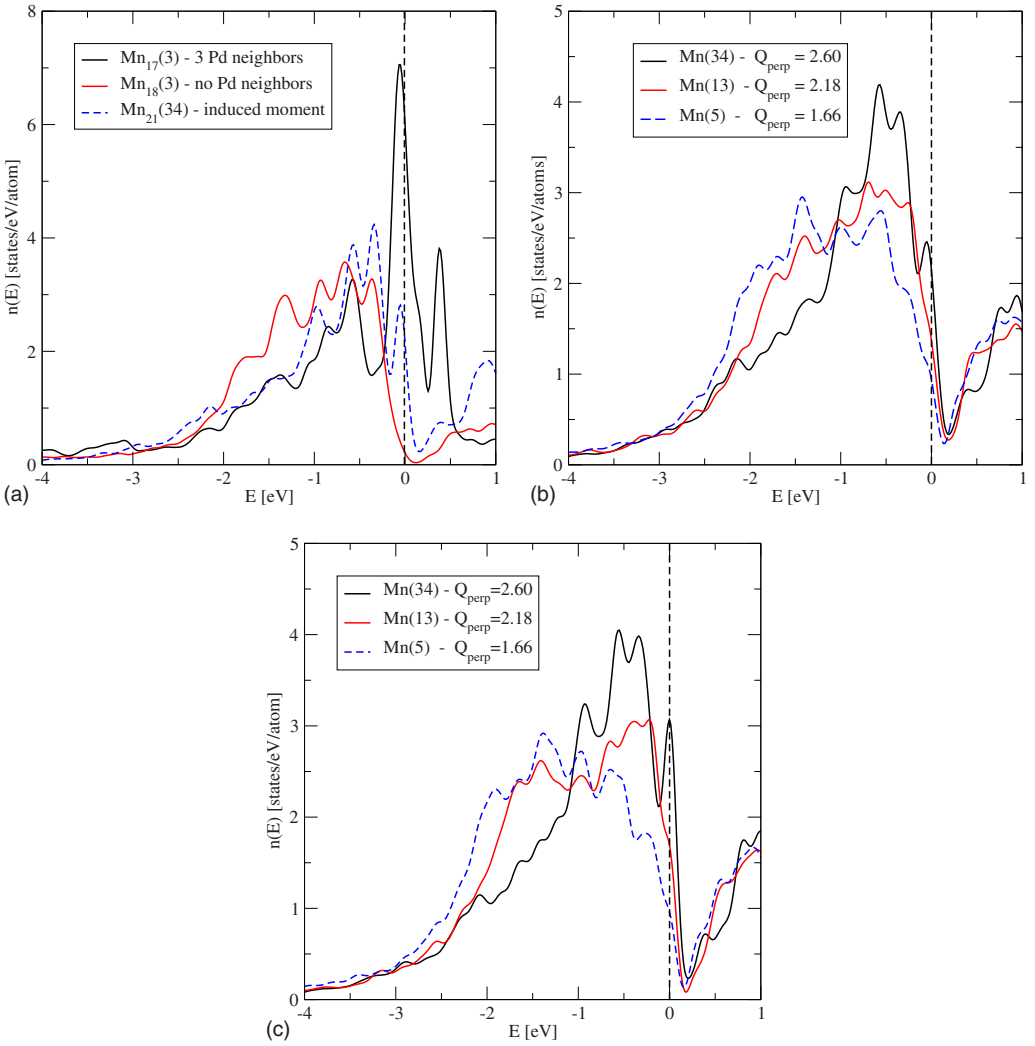

FIG. 14. (Color online) (a) The local paramagnetic d-DOS on the $Mn_{17}(3)$ atom with 3 Pd neighbors carrying the source magnetic moment in configuration P1, compared to that on the $Mn_{18}(3)$ atom from the same orbit (but no Pd neighbors), and with that on the $Mn_{21}(34)$ atom with the largest induced magnetic moment. (b) Local paramagnetic d-DOS's of three different Mn atoms with induced magnetic moments in configuration P1. The paramagnetic DOS at the Fermi level $n_d(E_F)$ increases with increasing perpendicular coordinate Q_{perp}. (c) Local paramagnetic DOS of three different Mn atoms with induced moments in configuration P2.

sites in i-Al-Pd-Mn quasicrystals and extended our studies to the fivefold surface of the quasicrystal. In our previous work[20] we have shown that within a large number of variants of the KGB model of i-Al-Pd-Mn differing in their chemical decorations the lowest energy is achieved after a slight modification of the shell structure of the triacontahedral occupation domains in the 6D hyperspace. In this ground-state configuration no Mn atom has a Pd atom in the nearest-neighbor shell, all Mn are nonmagnetic. Magnetic moments on Mn sites can be formed by two different physical mechanisms: (i) substitutional defects creating Mn-Pd nearest-neighbor pairs. Mn sites with two or three Pd atoms carry large magnetic moments. (ii) The creation of a loosely packed environment around a Mn atom.

Here we have demonstrated that Mn atoms located at the five-fold surface of i-Al-Pd-Mn are strongly magnetic, even if in the bulk the quasicrystal is completely nonmagnetic. The large magnetic moments at the surface Mn atoms are caused by their reduced coordination. Somewhat surprisingly, also Mn atoms at distances up to 10 Å from the surface carry smaller magnetic moments. These moments disappear if the strongly magnetic Mn atoms in the surface layers are replaced by Al. Hence the smaller magnetic moments found in the subsurface layers are clearly induced by a long-range interaction with the strongly magnetic surface atoms. However, the variation of the induced moments with their distance from the source moments looks at first a bit erratic, but we find a strong correlation between the size of the induced moment and the coordinate of the atom in 6D hyperspace.

In bulk i-Al-Pd-Mn we had also found large differences in the size of the magnetic moment, similar as between the source and induced moments close to the surface. However, as in our models retaining the full space-group symmetry of the 2/1 approximant, the same large moments exist always at all crystallographically equivalent (four or twelve) sites, it is very difficult to differentiate between source and induced moments. A further problem that had not been addressed in

our previous work is that the experimental studies yield a very large moment (between 6 and 7.5 μ_B, i.e., much larger than the limit set by Hund's rule for the magnetic moment of an isolated Mn atom) per magnetic Mn atom, while in our models the largest local moment did not exceed 3 μ_B.

Our earlier studies[20] have shown that for interpenetrating pseudo-Mackay (M) and Bergman (B) clusters connected along a three-fold symmetry axis, the chemical decoration of a site in the nearest-neighbor shell around the Mn atom in the center of the M cluster (which also belongs to the next-nearest-neighbor shell around the Pd atom in the B cluster) the decoration with Al or Pd is ill-defined with respect to the building principles of the clusters. At these sites substitution of Al by Pd or vice-versa leads only to small changes in the total energy. The ground state is achieved if these sites are occupied by Al, it is nonmagnetic. A magnetic moment on the Mn site is created if it has at least two Pd nearest neighbors. If a Mn(3) atom located in the center of a M cluster has three Pd neighbors (created by substituting Al), it acquires a large magnetic moment of 2.5 μ_B and induces smaller moments on a number of other sites at distances of up to 15 Å, the total magnetic moment is 6 μ_B. If a Mn(4) site in the center of the M cluster is surrounded by two Pd atoms, only a smaller local moment of about 0.5 μ_B is created, but the induced magnetic polarization adds up to a total effective moment of 8.4 μ_B. Thus we find: (i) substitutional Al/Pd defects close to Mn atoms cause the formation of a local magnetic moment, due to a mechanism based on the repulsive interaction between the d bands of the Mn and Pd atoms. (ii) The formation of the local moment induces a magnetic polarization of other Mn atoms over large distances, the effective magnetic moment per Mn atom is precisely of the order found in the experiments. The differences between these two particular cases is caused by a different local coordination [both Mn(3) and Mn(4) sites are located in the center of a M cluster and have an irregular first coordination shell, but Mn(3) has seven and Mn(4) nine Al neighbors] and to their coordination by highly polarizable Mn atoms. The polarizability of the Mn atoms has been found to be correlated with their coordinate in 6D hyperspace—the local DOS at the Fermi level and hence the polarizability increase with the perpendicular coordinate. As discussed above, the position of an atom within the occupation domain determines its local environment. The highly polarizable Mn(34) atoms are located at the extreme boundary between the Mn core and the Pd shell of the occupation domain—these sites could also be occupied by the larger Pd atoms, the nearest neighbors are located at relatively large distances.

The high magnetic polarizability of the Mn(34) sites relates to another mechanism for the formation of a local magnetic moment—a loosely packed environment around a Mn atom. We have discussed two possible realizations: (i) Relaxation of the nearest-neighbor shell is suppressed, and (ii) the packing density is reduced by the creation of a vacancy. The first mechanism is probably a bit academic—but it helps to understand the large response of the Mn(34) atoms. As these atoms sit in a loosely packed environment, their local DOS falls short of the Stoner limit for the formation of a magnetic moment. However, our earlier studies have shown that in this case some extra mechanism (e.g., a Mn next-nearest neighbor) is required to lead to a spontaneous local magnetization. Upon creation of a vacancy close to a Mn atom, relaxation distributes the created free volume over a larger environment. Thus only a small local moment on the Mn atom next to the vacancy is created, but at the same time smaller moments are created on a number of other sites. Hence the existence of structural vacancies leads to a diffuse magnetization providing a background to the large effective moments created by substitutional Pd/Al defects.

Together with our investigations of the physical mechanism leading to the formation of a pseudogap in the electronic spectrum[19] we have now a rather complete picture of the relationship between the structure and the electronic and magnetic properties of the icosahedral quasicrystals of the Al-Pd-Mn(Re) class: (i) the Katz-Gratias-Boudard model with triacontahedral occupation domains provides a good description of the quasicrystalline topology and a first-order approximation to the chemical order. (ii) For any calculation of the cohesive, electronic, and magnetic properties, a careful relaxation of the idealized model structure using interatomic forces calculated from first principles is required. The relaxation leads to a displacive modulation of the idealized structure. (iii) The existence of the characteristic pseudogap in the electronic spectrum is caused by the formation of a topological band gap in Al-TM chains connecting the centers of the pseudo-Mackay clusters building the quasicrystalline structure. The structural relaxation leads a dimerization of these chains with alternating short and long bonds which tends to widen the topologically induced pseudogap. The fragmentation of these chains by substitutional Al/Pd defects leads to the formation of localized electronic states within the pseudogap. (iv) The lowest energy is achieved for a chemical decoration in which some Pd atoms close to the triacontahedral surface separating the Pd and Al occupation domains at the odd vertices of the hypercubic lattice in 6D space are replaced by Al. This corresponds to the creation of phason defects such as they have been postulated on the basis of the analysis of the partial Pd structure factor.[2,21] (v) The ground-state configuration shows the deepest pseudogap, it is completely nonmagnetic. (vi) Large magnetic moments on Mn sites can be created by replacing at least two Al atoms in the nearest-neighbor shell of a Mn atom by Pd. Such substitutional defects can be created at very low energetic cost in the irregular first coordination shell around a Mn atom in the center of a pseudoMackay cluster. The large magnetic moments on these Mn atoms create a long-range magnetic polarization on other Mn atoms. These atoms carry smaller induced magnetic moments whose size varies as a function of the polarizability of the Mn (which depends on the local environment). (vii) Source moments created by one substitutional defect and induced moments together add up to a large effective moment per Mn atom, as observed in experiment. The effective moment is larger than the limit set by Hund's rule for the free Mn atom. (viii) The termination of the alternating Al-TM chains at a free surface causes a smearing of the pseudogap. (ix) The reduced coordination of the Mn atoms located at a surface of the quasicrystal leads to the formation of a large surface moment and further to the formation of smaller induced moments even rather deep in the bulk.

ACKNOWLEDGMENT

This work has been supported by the Austrian Ministry for Education, Science and Art through the Center for Computational Materials Science. M.K. thanks also for support from the Grant Agency for Science of Slovakia (Grant No. 2/5096/25) and from the Slovak Research and Development Agency (Grants No. APVV-0413-06, CEX-Nanosmart).

[1] D. Shechtman, I. Blech, D. Gratias, and J.-W. Cahn, Phys. Rev. Lett. **53**, 1951 (1984).
[2] M. de Boissieu, P. Stephens, M. Boudard, C. Janot, D. L. Chapman, and M. Audier, J. Phys.: Condens. Matter **6**, 10725 (1994).
[3] M. Mihalkovič, W.-J. Zhu, C. L. Henley, and M. Oxborrow, Phys. Rev. B **53**, 9002 (1996).
[4] A. P. Tsai, A. Inoue, and T. Masumoto, Philos. Mag. Lett. **62**, 95 (1990).
[5] M. Cornier-Quiquandon, A. Quivy, S. Lefebvre, E. Elkaim, G. Heger, A. Katz, and D. Gratias, Phys. Rev. B **44**, 2071 (1991).
[6] M. Boudard, M. de Boissieu, C. Janot, G. Heger, C. Beeli, H. U. Nissen, H. Vincent, R. Ibberson, M. Audier, and J. M. Dubois, J. Phys.: Condens. Matter **4**, 10149 (1992).
[7] A. Katz and D. Gratias, J. Non-Cryst. Solids **153-154**, 187 (1993).
[8] E. Cockayne, R. Phillips, X. B. Kan, S. C. Mos, J. L. Robertson, T. Ishimasa, and M. Mori, J. Non-Cryst. Solids **153-154**, 140 (1993).
[9] V. Elser, Philos. Mag. B **73**, 641 (1996).
[10] G. Kasner, Z. Papadopolos, P. Kramer, and D. E. Bürgler, Phys. Rev. B **60**, 3899 (1999).
[11] D. Gratias, F. Puyraimond, M. Quiquandon, and A. Katz, Phys. Rev. B **63**, 024202 (2000).
[12] M. Krajčí, M. Windisch, J. Hafner, G. Kresse, and M. Mihalkovič, Phys. Rev. B **51**, 17355 (1995).
[13] M. Krajčí and J. Hafner, Phys. Rev. B **68**, 165202 (2003).
[14] Ö. Rapp, in *Physical Properties of Quasicrystals*, edited by Z. M. Stadnik (Springer, Berlin, 1999), p. 127.
[15] V. Srinivas, M. Rodmar, S. J. Poon, and Ö. Rapp, Phys. Rev. B **63**, 172202 (2001).
[16] F. Hippert, M. Audier, J. J. Préjean, A. Sulpice, E. Lhotel, V. Simonet, and Y. Calvayrac, Phys. Rev. B **68**, 134402 (2003).
[17] C. A. Swenson, T. A. Lograsso, N. E. Anderson, Jr., and A. R. Ross, Phys. Rev. B **70**, 094201 (2004).
[18] F. Hippert, M. Audier, J. J. Préjean, A. Sulpice, V. Simonet, and Y. Calvayrac, J. Non-Cryst. Solids **334-335**, 403 (2004).
[19] M. Krajčí and J. Hafner, Phys. Rev. B **75**, 024116 (2007).
[20] M. Krajčí and J. Hafner, Phys. Rev. B **78**, 224207 (2008).
[21] M. de Boissieu, P. Stephens, M. Boudard, C. Janot, D. L. Chapman, and M. Audier, Phys. Rev. Lett. **72**, 3538 (1994).
[22] M. de Boissieu and S. Francoual, Z. Kristallogr. **220**, 1043 (2005).
[23] F. Hippert and J. J. Préjean, Philos. Mag., **88**, 1478 (2008).
[24] A. Sadoc and J. M. Dubois, J. Non-Cryst. Solids, **153-154**, 83 (1993).
[25] C. Berger and J. J. Préjean, Phys. Rev. Lett. **64**, 1769 (1990).
[26] K. Fukamichi, in *Physical Properties of Quasicrystals*, edited by Z. M. Stadnik, Solid State Sciences, Vol. 128 (Springer, Berlin 1999) p. 295.
[27] S. Dennler, J. Hafner, M. Marsman, and J. Morillo, Phys. Rev. B **71**, 094433 (2005).
[28] Yu. S. Dedkov, C. Laubschat, S. Khmelevskyi, J. Redinger, P. Mohn, and M. Weinert, Phys. Rev. Lett. **99**, 047204 (2007).
[29] M. Krajčí and J. Hafner, Phys. Rev. B **71**, 054202 (2005).
[30] M. Krajčí, J. Hafner, J. Ledieu, and R. McGrath, Phys. Rev. B **73**, 024202 (2006).
[31] M. Krajčí and J. Hafner, Phys. Rev. B **77**, 134202 (2008).
[32] B. Unal, V. Fournée, K. J. Schnitzenbaumer, C. Ghosh, C. J. Jenks, A. R. Ross, T. A. Lograsso, J. W. Evans, and P. A. Thiel, Phys. Rev. B **75**, 064205 (2007).
[33] G. Kresse and J. Hafner, Phys. Rev. B **49**, 14251 (1994).
[34] G. Kresse and J. Furthmüller, Comput. Mater. Sci. **6**, 15 (1996).
[35] G. Kresse and J. Furthmüller, Phys. Rev. B **54**, 11169 (1996).
[36] J. P. Perdew, J. A. Chevary, S. H. Vosko, K. A. Jackson, M. R. Pederson, D. J. Singh, and C. Fiolhais, Phys. Rev. B **46**, 6671 (1992).
[37] J. P. Perdew and Y. Wang, Phys. Rev. B **45**, 13244 (1992).
[38] S. H. Vosko, L. Wilk, and M. Nusair, Can. J. Phys. **58**, 1200 (1980).
[39] E. Belin, Z. Dankhazi, A. Sadoc, and J. M. Dubois, J. Phys.: Condens. Matter **6**, 8771 (1994).
[40] V. Fournée, P. J. Pinhero, J. W. Anderegg, T. A. Lograsso, A. R. Ross, P. C. Canfield, I. R. Fisher, and P. A. Thiel, Phys. Rev. B **62**, 14049 (2000).
[41] R. Widmer, P. Gröning, M. Feuerbacher, and O. Gröning, Phys. Rev. B **79**, 104202 (2009).
[42] V. Simonet, F. Hippert, H. Klein, M. Audier, R. Bellissent, H. Fischer, A. P. Murani, and D. Boursier, Phys. Rev. B **58**, 6273 (1998).
[43] J. Hafner and M. Krajčí, Phys. Rev. B **57**, 2849 (1998).
[44] N. Jakse and A. Pasturel, Phys. Rev. B **76**, 024207 (2007).
[45] Note that whether a node is even or odd depends on the choice of the coordinate. Some authors use a choice different from ours such even and odd are interchanged.